

8.1 Introduction

We saw earlier, in Section 1.9, that an isolated dynamical system consisting of two freely moving point masses exerting forces on one another—which is usually referred to as a *two-body problem*—can always be converted into an equivalent one-body problem. In particular, this implies that we can *exactly solve* a dynamical system containing two gravitationally interacting point masses, as the equivalent one-body problem is exactly soluble. (See Sections 1.9 and 3.16.) What about a system containing *three* gravitationally interacting point masses? Despite hundreds of years of research, no useful general solution of this famous problem—which is usually called the *three-body problem*—has ever been found. It is, however, possible to make some progress by severely restricting the problem’s scope.

8.2 Circular restricted three-body problem

Consider an isolated dynamical system consisting of three gravitationally interacting point masses, m_1 , m_2 , and m_3 . Suppose, however, that the third mass, m_3 , is so much smaller than the other two that it has a negligible effect on their motion. Suppose, further, that the first two masses, m_1 and m_2 , execute circular orbits about their common center of mass. In the following, we shall examine this simplified problem, which is usually referred to as the *circular restricted three-body problem*. The problem under investigation has obvious applications to the solar system. For instance, the first two masses might represent the Sun and a planet (recall that a given planet and the Sun do indeed execute almost circular orbits about their common center of mass), whereas the third mass might represent an asteroid or a comet (asteroids and comets do indeed have much smaller masses than the Sun or any of the planets).

Let us define a Cartesian coordinate system ξ , η , ζ in an inertial reference frame whose origin coincides with the center of mass, C , of the two orbiting masses, m_1 and m_2 . Furthermore, let the orbital plane of these masses coincide with the ξ – η plane, and let them both lie on the ξ -axis at time $t = 0$. (See Figure 8.1.) Suppose that a is the constant distance between the two orbiting masses, r_1 the constant distance between mass m_1 and the origin, and r_2 the constant distance between mass m_2 and the origin.

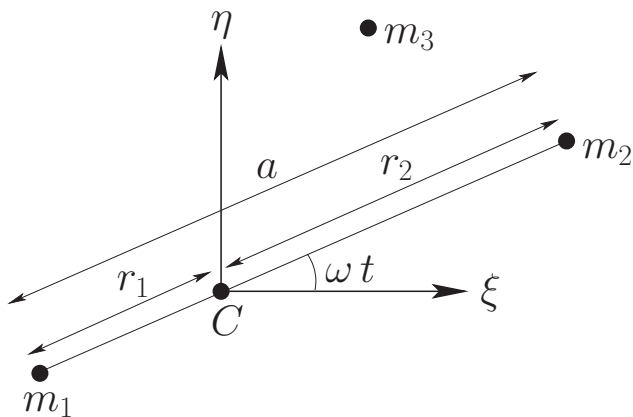


Fig. 8.1 Circular restricted three-body problem.

Moreover, let ω be the constant orbital angular velocity. It follows, from Section 3.16, that

$$\omega^2 = \frac{GM}{a^3} \quad (8.1)$$

and

$$\frac{r_1}{r_2} = \frac{m_2}{m_1}, \quad (8.2)$$

where $M = m_1 + m_2$.

It is convenient to choose our unit of length such that $a = 1$, and our unit of mass such that $GM = 1$. It follows, from Equation (8.1), that $\omega = 1$. However, we shall continue to retain ω in our equations, for the sake of clarity. Let $\mu_1 = Gm_1$ and $\mu_2 = Gm_2 = 1 - \mu_1$. It is easily demonstrated that $r_1 = \mu_2$ and $r_2 = 1 - r_1 = \mu_1$. Hence, the two orbiting masses, m_1 and m_2 , have position vectors

$$\mathbf{r}_1 = (\xi_1, \eta_1, 0) = (-\mu_2 \cos \omega t, -\mu_2 \sin \omega t, 0) \quad (8.3)$$

and

$$\mathbf{r}_2 = (\xi_2, \eta_2, 0) = (\mu_1 \cos \omega t, \mu_1 \sin \omega t, 0), \quad (8.4)$$

respectively. (See Figure 8.1.) Let the third mass have position vector $\mathbf{r} = (\xi, \eta, \zeta)$. The Cartesian components of the equation of motion of this mass are thus

$$\ddot{\xi} = -\mu_1 \frac{(\xi - \xi_1)}{\rho_1^3} - \mu_2 \frac{(\xi - \xi_2)}{\rho_2^3}, \quad (8.5)$$

$$\ddot{\eta} = -\mu_1 \frac{(\eta - \eta_1)}{\rho_1^3} - \mu_2 \frac{(\eta - \eta_2)}{\rho_2^3}, \quad (8.6)$$

$$\ddot{\zeta} = -\mu_1 \frac{\zeta}{\rho_1^3} - \mu_2 \frac{\zeta}{\rho_2^3}, \quad (8.7)$$

where

$$\rho_1^2 = (\xi - \xi_1)^2 + (\eta - \eta_1)^2 + \zeta^2 \quad (8.8)$$

and

$$\rho_2^2 = (\xi - \xi_2)^2 + (\eta - \eta_2)^2 + \zeta^2. \quad (8.9)$$

8.3 Jacobi integral

Consider the function

$$C = 2 \left(\frac{\mu_1}{\rho_1} + \frac{\mu_2}{\rho_2} \right) + 2 \omega (\xi \dot{\eta} - \eta \dot{\xi}) - \dot{\xi}^2 - \dot{\eta}^2 - \dot{\zeta}^2. \quad (8.10)$$

The time derivative of this function is written

$$\dot{C} = -\frac{2\mu_1\dot{\rho}_1}{\rho_1^2} - \frac{2\mu_2\dot{\rho}_2}{\rho_2^2} + 2\omega(\xi\ddot{\eta} - \eta\ddot{\xi}) - 2\dot{\xi}\ddot{\xi} - 2\dot{\eta}\ddot{\eta} - 2\dot{\zeta}\ddot{\zeta}. \quad (8.11)$$

Moreover, it follows, from Equations (8.3)–(8.4) and (8.8)–(8.9), that

$$\rho_1 \dot{\rho}_1 = -(\xi_1 \dot{\xi} + \eta_1 \dot{\eta}) + \omega(\xi \eta_1 - \eta \xi_1) + \xi \dot{\xi} + \eta \dot{\eta} + \zeta \dot{\zeta} \quad (8.12)$$

and

$$\rho_2 \dot{\rho}_2 = -(\xi_2 \dot{\xi} + \eta_2 \dot{\eta}) + \omega(\xi \eta_2 - \eta \xi_2) + \xi \dot{\xi} + \eta \dot{\eta} + \zeta \dot{\zeta}. \quad (8.13)$$

Combining Equations (8.5)–(8.7) with the preceding three expressions, after considerable algebra (see Exercise 8.1) we obtain

$$\frac{dC}{dt} = 0. \quad (8.14)$$

In other words, the function C —which is usually referred to as the *Jacobi integral*—is a *constant of the motion*.

We can rearrange Equation (8.10) to give

$$\mathcal{E} \equiv \frac{1}{2} (\dot{\xi}^2 + \dot{\eta}^2 + \dot{\zeta}^2) - \left(\frac{\mu_1}{\rho_1} + \frac{\mu_2}{\rho_2} \right) = \boldsymbol{\omega} \cdot \mathbf{h} - \frac{C}{2}, \quad (8.15)$$

where \mathcal{E} is the energy (per unit mass) of mass m_3 , $\mathbf{h} = \mathbf{r} \times \dot{\mathbf{r}}$ the angular momentum (per unit mass) of mass m_3 , and $\boldsymbol{\omega} = (0, 0, \omega)$ the orbital angular velocity of the other two masses. However, \mathbf{h} is *not* a constant of the motion. Hence, \mathcal{E} is not a constant of the motion either. In fact, the Jacobi integral is the *only* constant of the motion in the circular restricted three-body problem. Incidentally, the energy of mass m_3 is not a conserved quantity because the other two masses in the system are *moving*.

8.4 Tisserand criterion

Consider a dynamical system consisting of three gravitationally interacting point masses, m_1 , m_2 , and m_3 . Let mass m_1 represent the Sun, mass m_2 the planet Jupiter, and mass m_3 a comet. Because the mass of a comet is very much less than that of the

Sun or Jupiter, and the Sun and Jupiter are in (almost) circular orbits about their common center of mass, the dynamical system in question satisfies all the necessary criteria to be considered an example of a restricted three-body problem.

The mass of the Sun is much greater than that of Jupiter. It follows that the gravitational effect of Jupiter on the cometary orbit is *negligible* unless the comet makes a very close approach to Jupiter. Hence, as described in Chapter 3, before and after such an approach, the comet executes a Keplerian elliptical orbit about the Sun with fixed orbital parameters: fixed major radius, eccentricity, and inclination to the ecliptic plane. However, in general, the orbital parameters before and after the close approach will *not* be the same as one another. Let us investigate further.

Because $m_1 \gg m_2$, we have $\mu_1 = Gm_1 \approx G(m_1 + m_2) = 1$, and $\rho_1 \approx r$. Hence, according to Equations (3.34) and (3.44), the (approximately) conserved energy (per unit mass) of the comet before and after its close approach to Jupiter is

$$\mathcal{E} \equiv \frac{1}{2} (\dot{\xi}^2 + \dot{\eta}^2 + \dot{\zeta}^2) - \frac{1}{r} = -\frac{1}{2a}. \quad (8.16)$$

The comet's orbital energy is determined entirely by its major radius, a . (Incidentally, we are working in units such that the major radius of Jupiter's orbit is unity.) Furthermore, the (approximately) conserved angular momentum (per unit mass) of the comet before and after its approach to Jupiter is written \mathbf{h} , where \mathbf{h} is directed *normal* to the comet's orbital plane, and, from Equations (3.31) and (A.107),

$$h^2 = a(1 - e^2). \quad (8.17)$$

Here, e is the comet's orbital eccentricity. It follows that

$$\omega \cdot \mathbf{h} = \omega h \cos I = \sqrt{a(1 - e^2)} \cos I, \quad (8.18)$$

because $\omega = 1$ in our adopted system of units. Here, I is the angle of inclination of the normal to the comet's orbital plane to that of Jupiter's orbital plane.

Let a , e , and I be the major radius, eccentricity, and inclination angle of the cometary orbit before the close encounter with Jupiter, and let a' , e' , and I' be the corresponding parameters after the encounter. It follows from Equations (8.15), (8.16), and (8.18), and the fact that C is conserved during the encounter whereas \mathcal{E} and h are not, that

$$\frac{1}{2a} + \sqrt{a(1 - e^2)} \cos I = \frac{1}{2a'} + \sqrt{a'(1 - e'^2)} \cos I'. \quad (8.19)$$

This result is known as the *Tisserand criterion* after its discoverer, the French astronomer Felix Tisserand (1845–1896); it restricts the possible changes in the orbital parameters of a comet due to a close encounter with Jupiter (or any other massive planet).

The Tisserand criterion is extremely useful. For instance, whenever a new comet is discovered, astronomers immediately calculate its *Tisserand parameter*,

$$T_J = \frac{1}{a} + 2 \sqrt{a(1 - e^2)} \cos I. \quad (8.20)$$

If this parameter has the same value as that of a previously observed comet, it is quite likely that the new comet is, in fact, the same comet, but that its orbital parameters have changed since it was last observed, as a result of a close encounter with Jupiter. Incidentally, the subscript J in the preceding formula is to remind us that we are dealing

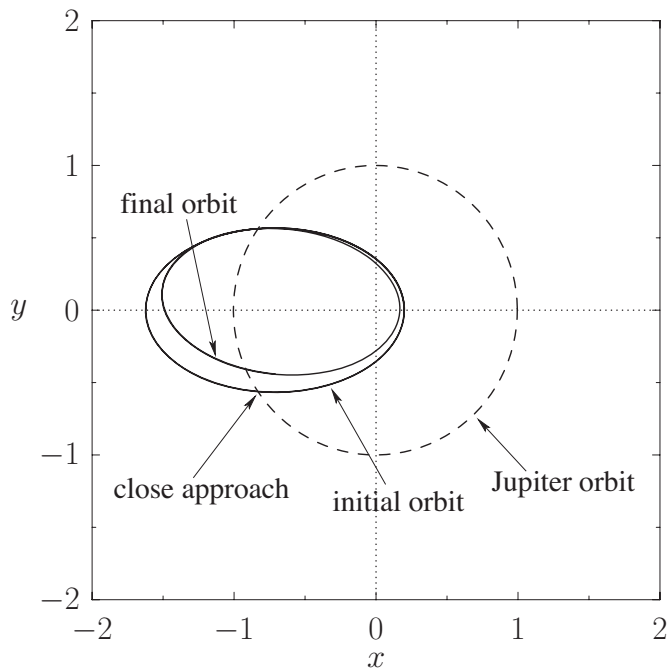


Fig. 8.2 Changing orbit of a hypothetical comet with a close approach to Jupiter. The solid curve shows the cometary orbit, and the dashed curve shows the jovian orbit. x and y are Cartesian coordinates in Jupiter's orbital plane. The origin is the center of mass of the Sun–Jupiter system. The system of units is such that the Jovian major radius is unity, and $\mu_2 = 9.533 \times 10^{-4}$. Both the comet and Jupiter orbit in a counterclockwise sense.

with the Tisserand parameter for close encounters with Jupiter. (The parameter is thus evaluated in a system of units in which the major radius of Jupiter's orbit is unity.) Obviously, it is also possible to calculate Tisserand parameters for close encounters with other massive planets.

Figure 8.2 shows the changing orbit of a hypothetical comet that has a close approach to Jupiter. The initial orbit is such that $a = 0.916$ (in units in which the major radius of the Jovian orbit is unity), $e = 0.781$, and $I = 0$, whereas the final orbit is such that $a = 0.841$, $e = 0.800$, and $I = 0$. Figure 8.3 shows the comet's major radius, a , eccentricity, e , and Tisserand parameter, T_J , as functions of time before, during, and after the encounter with Jupiter. It can be seen that the major radius and the eccentricity are both modified by the encounter (which occurs when $t \approx 12$), whereas the Tisserand parameter remains constant in time. This remains true even when the small eccentricity of the Jovian orbit is taken into account in the calculation.

The Tisserand parameter is often employed to distinguish between comets and asteroids in the solar system. This idea is illustrated in Figure 8.4, which shows the Jovian Tisserand parameter, T_J , plotted against the major radius, a , of the principal asteroids and comets in the solar system. The Tisserand parameter of Jupiter (which is almost exactly 3) is also shown. It can be seen that, roughly speaking, asteroids have higher Tisserand parameters than Jupiter, whereas comets have lower Tisserand parameters. The only major exception to this rule is the so-called *Trojan asteroids* (see Section 8.8),

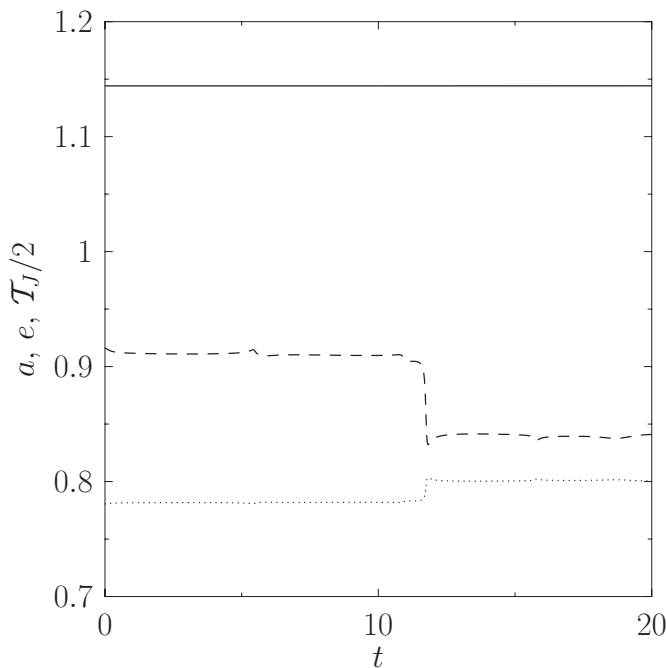


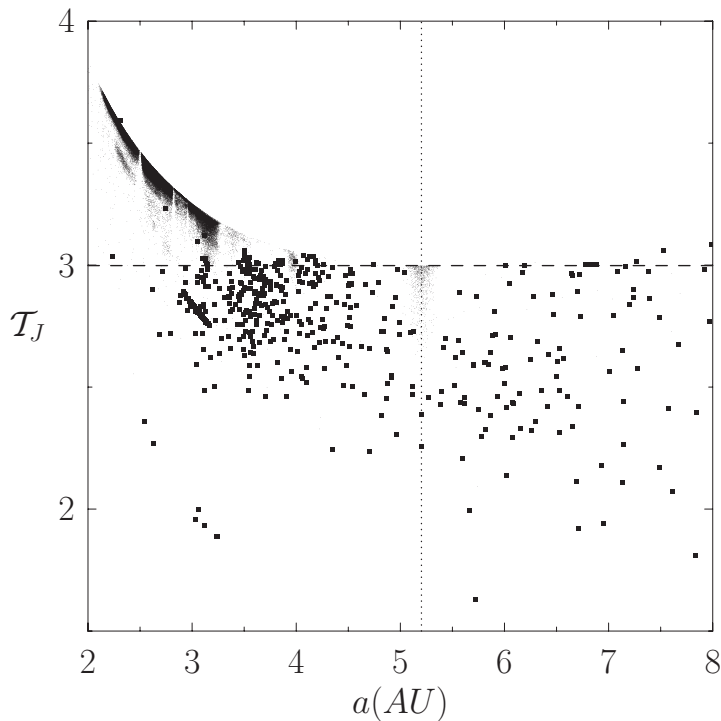
Fig. 8.3 Major radius, a (dashed curve) and eccentricity, e (dotted curve) of the hypothetical comet shown in Figure 8.2, plotted as functions of time. The adopted system of units is such that the Jovian major radius and orbital period are both unity. The solid curve shows the comet's Tisserand parameter, T_J , divided by 2.

which all have very similar major radii to Jupiter (because, by definition, they must have the same orbital period as Jupiter), and consequently have lower Tisserand parameters (because they generally have higher eccentricities and inclinations than Jupiter). The lower Tisserand parameters of comets with respect to Jupiter, and of Jupiter with respect to regular asteroids, is indicative of the fact that comets generally originated *beyond* the Jovian orbit, whereas regular asteroids generally originated *within* the Jovian orbit.

The Tisserand criterion is also applicable to so-called *gravity assists*, in which a spacecraft gains energy as a result of a close encounter with a moving planet. Such assists are often employed in missions to the outer planets to reduce the amount of fuel that the spacecraft must carry in order to reach its destination. In fact, it is clear, from Equations (8.16) and (8.19), that a spacecraft can make use of a close encounter with a moving planet to increase (or decrease) its orbital major radius a , and, hence, to increase (or decrease) its total orbital energy.

8.5 Co-rotating frame

Let us transform to a noninertial frame of reference rotating with angular velocity ω about an axis normal to the orbital plane of masses m_1 and m_2 , and passing through their center of mass. It follows that masses m_1 and m_2 appear stationary in this new

**Fig. 8.4**

Jovian Tisserand parameter versus major radius for all the principal asteroids (dots) and comets (squares) in the solar system. The dashed line indicates the Tisserand parameter of Jupiter. The dotted line shows the Jovian major radius. Raw data from JPL Small-Body Database.

reference frame. Let us define a Cartesian coordinate system x , y , z in the rotating frame of reference that is such that masses m_1 and m_2 always lie on the x -axis, and the z -axis is parallel to the previously defined ζ -axis. It follows that masses m_1 and m_2 have the fixed position vectors $\mathbf{r}_1 = (-\mu_2, 0, 0)$ and $\mathbf{r}_2 = (\mu_1, 0, 0)$ in our new coordinate system. Finally, let the position vector of mass m_3 be $\mathbf{r} = (x, y, z)$. (See Figure 8.5.)

According to Section 5.2, the equation of motion of mass m_3 in the rotating reference frame takes the form

$$\ddot{\mathbf{r}} + 2\boldsymbol{\omega} \times \dot{\mathbf{r}} = -\mu_1 \frac{(\mathbf{r} - \mathbf{r}_1)}{\rho_1^3} - \mu_2 \frac{(\mathbf{r} - \mathbf{r}_2)}{\rho_2^3} - \boldsymbol{\omega} \times (\boldsymbol{\omega} \times \mathbf{r}), \quad (8.21)$$

where $\boldsymbol{\omega} = (0, 0, \omega)$, and

$$\rho_1^2 = (x + \mu_2)^2 + y^2 + z^2, \quad (8.22)$$

$$\rho_2^2 = (x - \mu_1)^2 + y^2 + z^2. \quad (8.23)$$

Here, the second term on the left-hand side of Equation (8.21) is the *Coriolis* acceleration, whereas the final term on the right-hand side is the *centrifugal* acceleration.

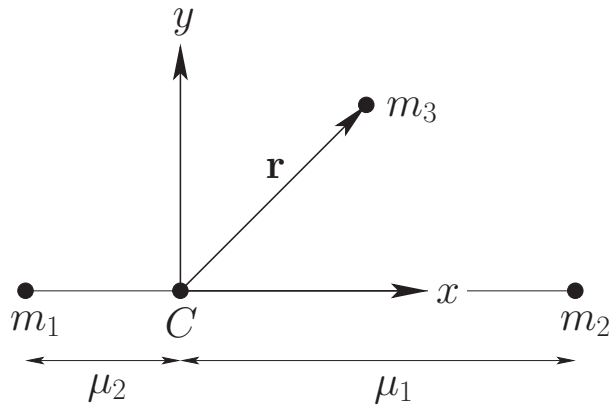


Fig. 8.5 Co-rotating frame.

The components of Equation (8.21) reduce to

$$\ddot{x} - 2\omega \dot{y} = -\frac{\mu_1(x + \mu_2)}{\rho_1^3} - \frac{\mu_2(x - \mu_1)}{\rho_2^3} + \omega^2 x, \quad (8.24)$$

$$\ddot{y} + 2\omega \dot{x} = -\frac{\mu_1 y}{\rho_1^3} - \frac{\mu_2 y}{\rho_2^3} + \omega^2 y, \quad (8.25)$$

and

$$\ddot{z} = -\frac{\mu_1 z}{\rho_1^3} - \frac{\mu_2 z}{\rho_2^3}, \quad (8.26)$$

which yield

$$\ddot{x} - 2\omega \dot{y} = -\frac{\partial U}{\partial x}, \quad (8.27)$$

$$\ddot{y} + 2\omega \dot{x} = -\frac{\partial U}{\partial y}, \quad (8.28)$$

and

$$\ddot{z} = -\frac{\partial U}{\partial z}, \quad (8.29)$$

where

$$U(x, y, z) = -\frac{\mu_1}{\rho_1} - \frac{\mu_2}{\rho_2} - \frac{\omega^2}{2}(x^2 + y^2) \quad (8.30)$$

is the sum of the gravitational and centrifugal potentials.

It follows from Equations (8.27)–(8.29) that

$$\ddot{x} \dot{x} - 2\omega \dot{x} \dot{y} = -\dot{x} \frac{\partial U}{\partial x}, \quad (8.31)$$

$$\ddot{y} \dot{y} + 2\omega \dot{x} \dot{y} = -\dot{y} \frac{\partial U}{\partial y}, \quad (8.32)$$

and

$$\ddot{z} \dot{z} = -\dot{z} \frac{\partial U}{\partial z}. \quad (8.33)$$

Summing the preceding three equations, we obtain

$$\frac{d}{dt} \left[\frac{1}{2} (\dot{x}^2 + \dot{y}^2 + \dot{z}^2) + U \right] = 0. \quad (8.34)$$

In other words,

$$C = -2U - v^2 \quad (8.35)$$

is a *constant of the motion*, where $v^2 = \dot{x}^2 + \dot{y}^2 + \dot{z}^2$. In fact, C is the *Jacobi integral* introduced in Section 8.3 [it is easily demonstrated that Equations (8.10) and (8.35) are identical—see Exercise 8.4]. Note, finally, that the mass m_3 is restricted to regions in which

$$-2U \geq C, \quad (8.36)$$

because v^2 is a positive definite quantity.

8.6 Lagrange points

Let us search for possible *equilibrium points* of the mass m_3 in the rotating reference frame. Such points are termed *Lagrange points*. Hence, in the rotating frame, the mass m_3 would remain at rest if placed at one of the Lagrange points. It is thus clear that these points are fixed in the rotating frame. Conversely, in the inertial reference frame, the Lagrange points rotate about the center of mass with angular velocity ω , and the mass m_3 would consequently also rotate about the center of mass with angular velocity ω if placed at one of these points (with the appropriate velocity). In the following, we shall assume, without loss of generality, that $m_1 \geq m_2$.

The Lagrange points satisfy $\dot{\mathbf{r}} = \ddot{\mathbf{r}} = \mathbf{0}$ in the rotating frame. It thus follows, from Equations (8.27)–(8.29), that the Lagrange points are the solutions of

$$\frac{\partial U}{\partial x} = \frac{\partial U}{\partial y} = \frac{\partial U}{\partial z} = 0. \quad (8.37)$$

It is easily seen that

$$\frac{\partial U}{\partial z} = \left(\frac{\mu_1}{\rho_1^3} + \frac{\mu_2}{\rho_2^3} \right) z. \quad (8.38)$$

Because the term in curved brackets is positive definite, we conclude that the only solution to the above equation is $z = 0$. Hence, all the Lagrange points lie in the x – y plane.

If $z = 0$, it is readily demonstrated that

$$\mu_1 \rho_1^2 + \mu_2 \rho_2^2 = x^2 + y^2 + \mu_1 \mu_2, \quad (8.39)$$

where use has been made of the fact that $\mu_1 + \mu_2 = 1$. Hence, Equation (8.30) can also be written

$$U = -\mu_1 \left(\frac{1}{\rho_1} + \frac{\rho_1^2}{2} \right) - \mu_2 \left(\frac{1}{\rho_2} + \frac{\rho_2^2}{2} \right) + \frac{\mu_1 \mu_2}{2}. \quad (8.40)$$

The Lagrange points thus satisfy

$$\frac{\partial U}{\partial x} = \frac{\partial U}{\partial \rho_1} \frac{\partial \rho_1}{\partial x} + \frac{\partial U}{\partial \rho_2} \frac{\partial \rho_2}{\partial x} = 0 \quad (8.41)$$

and

$$\frac{\partial U}{\partial y} = \frac{\partial U}{\partial \rho_1} \frac{\partial \rho_1}{\partial y} + \frac{\partial U}{\partial \rho_2} \frac{\partial \rho_2}{\partial y} = 0, \quad (8.42)$$

which reduce to

$$\mu_1 \left(\frac{1 - \rho_1^3}{\rho_1^2} \right) \left(\frac{x + \mu_2}{\rho_1} \right) + \mu_2 \left(\frac{1 - \rho_2^3}{\rho_2^2} \right) \left(\frac{x - \mu_1}{\rho_2} \right) = 0 \quad (8.43)$$

and

$$\mu_1 \left(\frac{1 - \rho_1^3}{\rho_1^2} \right) \left(\frac{y}{\rho_1} \right) + \mu_2 \left(\frac{1 - \rho_2^3}{\rho_2^2} \right) \left(\frac{y}{\rho_2} \right) = 0. \quad (8.44)$$

One obvious solution of Equation (8.44) is $y = 0$, corresponding to a Lagrange point that lies on the x -axis. It turns out that there are three such points. L_1 lies between masses m_1 and m_2 , L_2 lies to the right of mass m_2 , and L_3 lies to the left of mass m_1 . (See Figure 8.5.) At the L_1 point, we have $x = -\mu_2 + \rho_1 = \mu_1 - \rho_2$ and $\rho_1 = 1 - \rho_2$. Hence, from Equation (8.43),

$$\frac{\mu_2}{3\mu_1} = \frac{\rho_2^3(1 - \rho_2 + \rho_2^2/3)}{(1 + \rho_2 + \rho_2^2)(1 - \rho_2)^3}. \quad (8.45)$$

Assuming that $\rho_2 \ll 1$, we can find an approximate solution of Equation (8.45) by expanding in powers of ρ_2 :

$$\alpha = \rho_2 + \frac{\rho_2^2}{3} + \frac{\rho_2^3}{3} + \frac{53\rho_2^4}{81} + \mathcal{O}(\rho_2^5). \quad (8.46)$$

This equation can be inverted to give

$$\rho_2 = \alpha - \frac{\alpha^2}{3} - \frac{\alpha^3}{9} - \frac{23\alpha^4}{81} + \mathcal{O}(\alpha^5), \quad (8.47)$$

where

$$\alpha = \left(\frac{\mu_2}{3\mu_1} \right)^{1/3} \quad (8.48)$$

is assumed to be a small parameter.

At the L_2 point, we have $x = -\mu_2 + \rho_1 = \mu_1 + \rho_2$ and $\rho_1 = 1 + \rho_2$. Hence, from Equation (8.43),

$$\frac{\mu_2}{3\mu_1} = \frac{\rho_2^3(1 + \rho_2 + \rho_2^2/3)}{(1 + \rho_2)^2(1 - \rho_2^3)}. \quad (8.49)$$

Again, expanding in powers of ρ_2 , we obtain

$$\alpha = \rho_2 - \frac{\rho_2^2}{3} + \frac{\rho_2^3}{3} + \frac{\rho_2^4}{81} + \mathcal{O}(\rho_2^5) \quad (8.50)$$

and

$$\rho_2 = \alpha + \frac{\alpha^2}{3} - \frac{\alpha^3}{9} - \frac{31\alpha^4}{81} + \mathcal{O}(\alpha^5). \quad (8.51)$$

Finally, at the L_3 point, we have $x = -\mu_2 - \rho_1 = \mu_1 - \rho_2$ and $\rho_2 = 1 + \rho_1$. Hence, from Equation (8.43),

$$\frac{\mu_2}{\mu_1} = \frac{(1 - \rho_1^3)(1 + \rho_1)^2}{\rho_1^3(\rho_1^2 + 3\rho_1 + 3)}. \quad (8.52)$$

Let $\rho_1 = 1 - \beta$. Expanding in powers of β , we obtain

$$\frac{\mu_2}{\mu_1} = \frac{12\beta}{7} + \frac{144\beta^2}{49} + \frac{1567\beta^3}{343} + \mathcal{O}(\beta^4) \quad (8.53)$$

and

$$\beta = \frac{7}{12} \left(\frac{\mu_2}{\mu_1} \right) - \frac{7}{12} \left(\frac{\mu_2}{\mu_1} \right)^2 + \frac{13223}{20736} \left(\frac{\mu_2}{\mu_1} \right)^3 + \mathcal{O} \left(\frac{\mu_2}{\mu_1} \right)^4, \quad (8.54)$$

where μ_2/μ_1 is assumed to be a small parameter.

Let us now search for Lagrange points that *do not* lie on the x -axis. One obvious solution of Equations (8.41) and (8.42) is

$$\frac{\partial U}{\partial \rho_1} = \frac{\partial U}{\partial \rho_2} = 0, \quad (8.55)$$

giving, from Equation (8.40),

$$\rho_1 = \rho_2 = 1 \quad (8.56)$$

or

$$(x + \mu_2)^2 + y^2 = (x - 1 + \mu_2)^2 + y^2 = 1, \quad (8.57)$$

because $\mu_1 = 1 - \mu_2$. The two solutions of this equation are

$$x = \frac{1}{2} - \mu_2 \quad (8.58)$$

and

$$y = \pm \frac{\sqrt{3}}{2}, \quad (8.59)$$

and they specify the positions of the Lagrange points designated L_4 and L_5 . Note that the point L_4 and the masses m_1 and m_2 lie at the apexes of an *equilateral triangle*. The same is true for the point L_5 . We have now found all of the possible Lagrange points.

Figure 8.6 shows the positions of the two masses, m_1 and m_2 , and the five Lagrange points, L_1 to L_5 , calculated for the case where $\mu_2 = 0.1$.

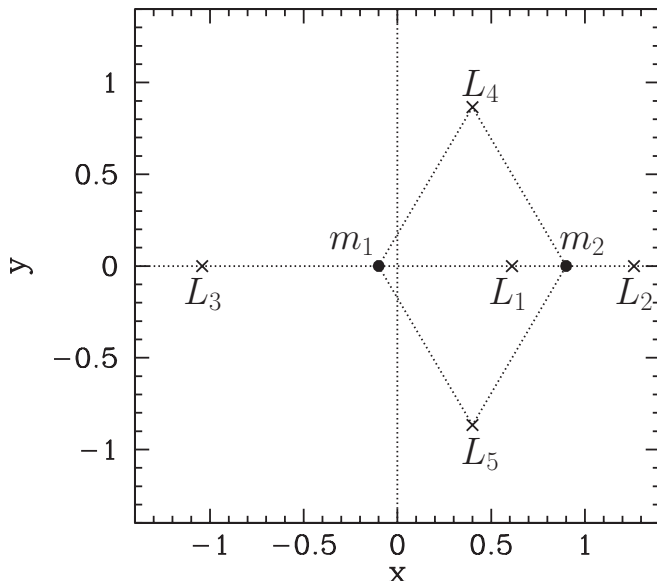


Fig. 8.6 Masses m_1 and m_2 , and the five Lagrange points, L_1 to L_5 , calculated for $\mu_2 = 0.1$.

8.7 Zero-velocity surfaces

Consider the surface

$$V(x, y, z) = C, \quad (8.60)$$

where

$$V(x, y, z) = -2U = \frac{2\mu_1}{\rho_1} + \frac{2\mu_2}{\rho_2} + x^2 + y^2. \quad (8.61)$$

Note that $V \geq 0$. It follows, from Equation (8.35), that if the mass m_3 has the Jacobi integral C and lies on the surface specified in Equation (8.60), then it must have zero velocity. Hence, such a surface is termed a *zero-velocity surface*. The zero-velocity surfaces are important because they form the boundary of regions from which the mass m_3 is dynamically excluded: that is, regions where $V < C$. Generally speaking, the regions from which m_3 is excluded, grow in area as C increases, and vice versa.

Let C_i be the value of V at the L_i Lagrange point, for $i = 1, 5$. When $\mu_2 \ll 1$, it is easily demonstrated that

$$C_1 \approx 3 + 3^{4/3} \mu_2^{2/3} - 10\mu_2/3, \quad (8.62)$$

$$C_2 \approx 3 + 3^{4/3} \mu_2^{2/3} - 14\mu_2/3, \quad (8.63)$$

$$C_3 \approx 3 + \mu_2, \quad (8.64)$$

$$C_4 \approx 3 - \mu_2, \quad (8.65)$$

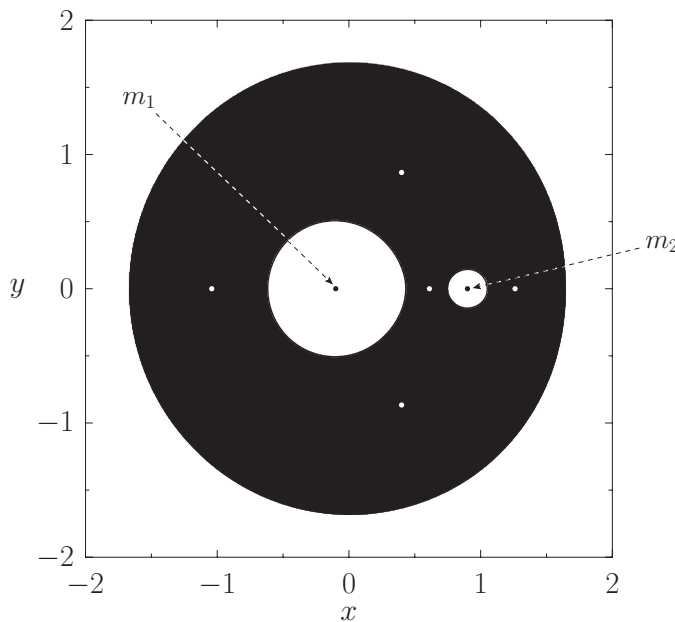


Fig. 8.7 Zero-velocity surface $V = C$, where $C > C_1$, calculated for $\mu_2 = 0.1$. Mass m_3 is excluded from the black region.

and

$$C_5 \simeq 3 - \mu_2. \quad (8.66)$$

Note that $C_1 > C_2 > C_3 > C_4 = C_5$.

Figures 8.7 through 8.11 show the intersection of the zero-velocity surface $V = C$ with the x - y plane for various different values of C , and illustrate how the region from which m_3 is dynamically excluded—which we shall term the *excluded region*—evolves as the value of C is varied. Of course, any point not in the excluded region is in the so-called *allowed region*. For $C > C_1$, the allowed region consists of two separate oval regions centered on m_1 and m_2 , respectively, plus an outer region that lies beyond a large circle centered on the origin. All three allowed regions are separated from one another by an excluded region. (See Figure 8.7.) When $C = C_1$, the two inner allowed regions merge at the L_1 point. (See Figure 8.8.) When $C = C_2$, the inner and outer allowed regions merge at the L_2 point, forming a horseshoe-like excluded region. (See Figure 8.9.) When $C = C_3$, the excluded region splits in two at the L_3 point. (See Figure 8.10.) For $C_4 < C < C_3$, the two excluded regions are localized about the L_4 and L_5 points. (See Figure 8.11.) Finally, for $C < C_4$, there is no excluded region.

Figure 8.12 shows the zero-velocity surfaces and Lagrange points calculated for the case $\mu_2 = 0.01$. It can be seen that, at very small values of μ_2 , the L_1 and L_2 Lagrange points are almost equidistant from mass m_2 . Furthermore, mass m_2 and the L_3 , L_4 , and L_5 Lagrange points all lie approximately on a *unit circle*, centered on mass m_1 . It follows that, when μ_2 is small, the Lagrange points L_3 , L_4 and L_5 all share the orbit of mass m_2 .

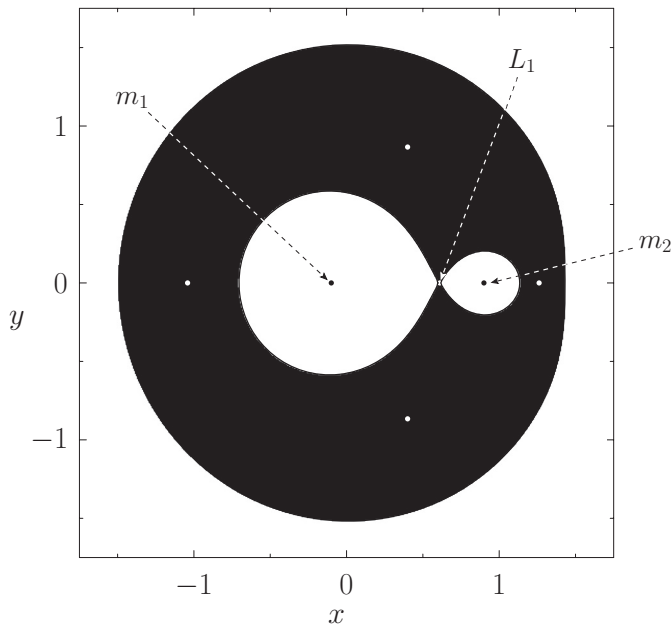


Fig. 8.8 Zero-velocity surface $V = C$, where $C = C_1$, calculated for $\mu_2 = 0.1$. Mass m_3 is excluded from the black region.

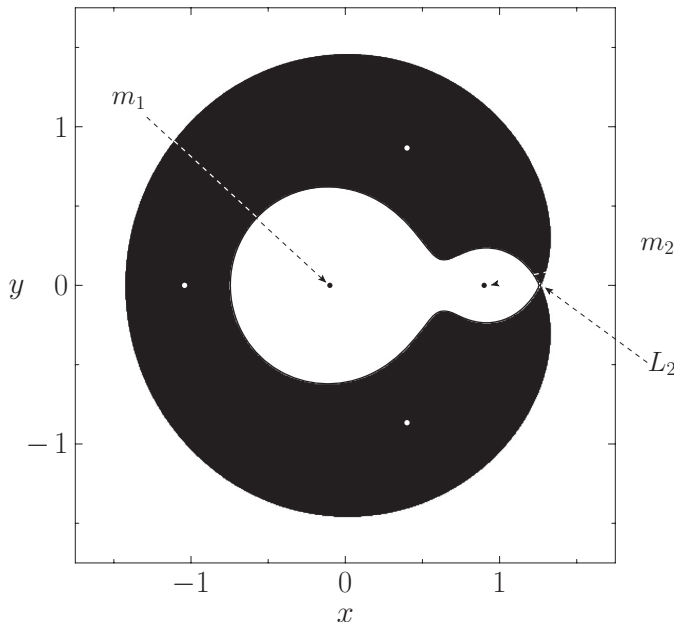


Fig. 8.9 Zero-velocity surface $V = C$, where $C = C_2$, calculated for $\mu_2 = 0.1$. Mass m_3 is excluded from the black region.

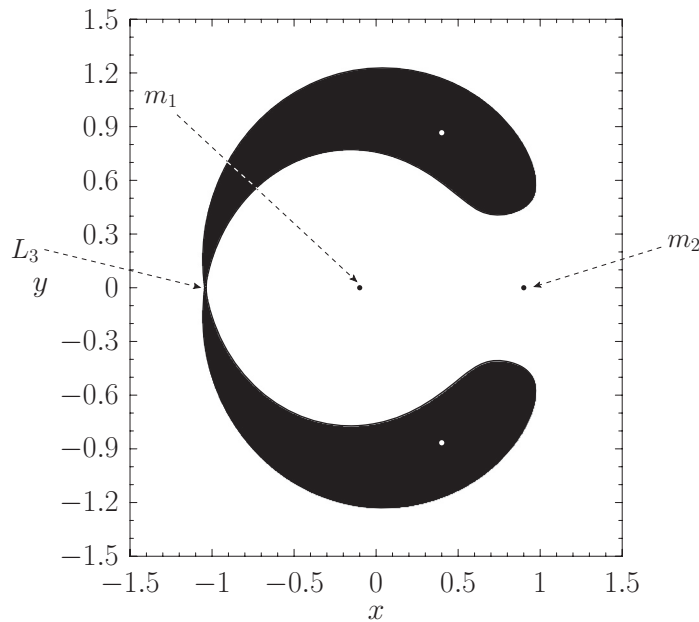


Fig. 8.10 Zero-velocity surface $V = C$, where $C = C_3$, calculated for $\mu_2 = 0.1$. Mass m_3 is excluded from the black region.

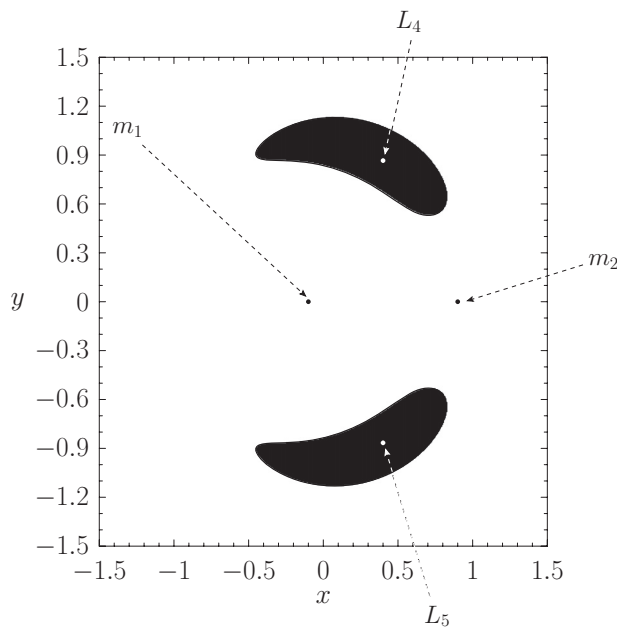


Fig. 8.11 Zero-velocity surface $V = C$, where $C_4 < C < C_3$, calculated for $\mu_2 = 0.1$. Mass m_3 is excluded from the black regions.

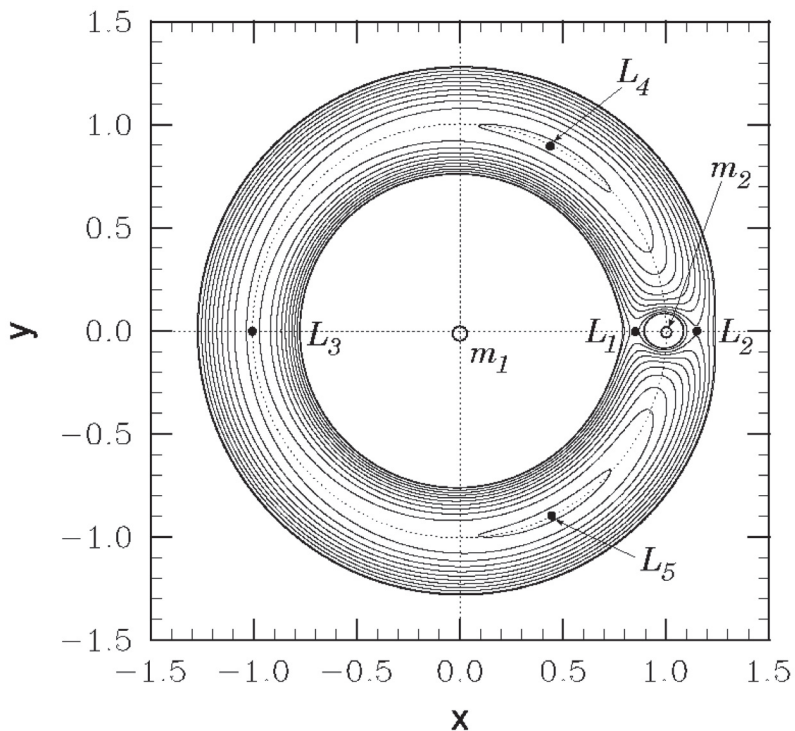


Fig. 8.12 Zero-velocity surfaces and Lagrange points calculated for $\mu_2 = 0.01$.

about m_1 (in the inertial frame) with L_3 being directly opposite m_2 , L_4 (by convention) 60° ahead of m_2 , and L_5 60° behind.

8.8 Stability of Lagrange points

We have seen that the five Lagrange points, L_1 to L_5 , are the equilibrium points of mass m_3 in the co-rotating frame. Let us now determine whether these equilibrium points are stable to small displacements.

The equations of motion of mass m_3 in the co-rotating frame are specified in Equations (8.27)–(8.29). The motion in the x - y plane is complicated by presence of the Coriolis acceleration. However, the motion parallel to the z -axis simply corresponds to motion in the potential U . Hence, the condition for the stability of the Lagrange points (which all lie at $z = 0$) to small displacements parallel to the z -axis is simply (see Section 1.7)

$$\left(\frac{\partial^2 U}{\partial z^2}\right)_{z=0} = \frac{\mu_1}{\rho_1^3} + \frac{\mu_2}{\rho_2^3} > 0. \quad (8.67)$$

This condition is satisfied everywhere in the x - y plane. Hence, the Lagrange points are all stable to small displacements parallel to the z -axis. It thus remains to investigate their stability to small displacements lying within the x - y plane.

Suppose that a Lagrange point is situated in the x - y plane at coordinates $(x_0, y_0, 0)$. Let us consider small amplitude x - y motion in the vicinity of this point by writing

$$x = x_0 + \delta x, \quad (8.68)$$

$$y = y_0 + \delta y, \quad (8.69)$$

and

$$z = 0, \quad (8.70)$$

where δx and δy are infinitesimal. Expanding $U(x, y, 0)$ about the Lagrange point as a Taylor series, and retaining terms up to second order in small quantities, we obtain

$$U \approx U_0 + U_x \delta x + U_y \delta y + \frac{1}{2} U_{xx} (\delta x)^2 + U_{xy} \delta x \delta y + \frac{1}{2} U_{yy} (\delta y)^2, \quad (8.71)$$

where $U_0 = U(x_0, y_0, 0)$, $U_x = \partial U(x_0, y_0, 0)/\partial x$, $U_{xx} = \partial^2 U(x_0, y_0, 0)/\partial x^2$, and so on. However, by definition, $U_x = U_y = 0$ at a Lagrange point, so the expansion simplifies to

$$U \approx U_0 + \frac{1}{2} U_{xx} (\delta x)^2 + U_{xy} \delta x \delta y + \frac{1}{2} U_{yy} (\delta y)^2. \quad (8.72)$$

Finally, substituting Equations (8.68)–(8.70) and (8.72) into the equations of x - y motion, (8.27) and (8.28), and only retaining terms up to first order in small quantities, we get

$$\delta \ddot{x} - 2 \delta \dot{y} \approx -U_{xx} \delta x - U_{xy} \delta y \quad (8.73)$$

and

$$\delta \ddot{y} + 2 \delta \dot{x} \approx -U_{xy} \delta x - U_{yy} \delta y, \quad (8.74)$$

as $\omega = 1$.

Let us search for a solution of the preceding pair of equations of the form $\delta x(t) = \delta x_0 \exp(\gamma t)$ and $\delta y(t) = \delta y_0 \exp(\gamma t)$. We obtain

$$\begin{pmatrix} \gamma^2 + U_{xx} & -2\gamma + U_{xy} \\ 2\gamma + U_{xy} & \gamma^2 + U_{yy} \end{pmatrix} \begin{pmatrix} \delta x_0 \\ \delta y_0 \end{pmatrix} = \begin{pmatrix} 0 \\ 0 \end{pmatrix}. \quad (8.75)$$

This equation only has a nontrivial solution if the determinant of the matrix is zero. Hence, we get

$$\gamma^4 + (4 + U_{xx} + U_{yy}) \gamma^2 + (U_{xx} U_{yy} - U_{xy}^2) = 0. \quad (8.76)$$

It is convenient to define

$$A = \frac{\mu_1}{\rho_1^3} + \frac{\mu_2}{\rho_2^3}, \quad (8.77)$$

$$B = 3 \left[\frac{\mu_1}{\rho_1^5} + \frac{\mu_2}{\rho_2^5} \right] y^2, \quad (8.78)$$

$$C = 3 \left[\frac{\mu_1(x + \mu_2)}{\rho_1^5} + \frac{\mu_2(x - \mu_1)}{\rho_2^5} \right] y, \quad (8.79)$$

and

$$D = 3 \left[\frac{\mu_1(x + \mu_2)^2}{\rho_1^5} + \frac{\mu_2(x - \mu_1)^2}{\rho_2^5} \right], \quad (8.80)$$

where all terms are evaluated at the point $(x_0, y_0, 0)$. It thus follows that

$$U_{xx} = A - D - 1, \quad (8.81)$$

$$U_{yy} = A - B - 1, \quad (8.82)$$

and

$$U_{xy} = -C. \quad (8.83)$$

Consider the co-linear Lagrange points, L_1 , L_2 , and L_3 . These all lie on the x -axis, and are thus characterized by $y = 0$, $\rho_1^2 = (x + \mu_2)^2$, and $\rho_2^2 = (x - \mu_1)^2$. It follows, from the preceding equations, that $B = C = 0$ and $D = 3A$. Hence, $U_{xx} = -1 - 2A$, $U_{yy} = A - 1$, and $U_{xy} = 0$. Equation (8.76) thus yields

$$\Gamma^2 + (2 - A)\Gamma + (1 - A)(1 + 2A) = 0, \quad (8.84)$$

where $\Gamma = \gamma^2$. For a Lagrange point to be stable to small displacements, all four of the roots, γ , of Equation (8.76) must be *purely imaginary*. This, in turn, implies that the two roots of the preceding equation,

$$\Gamma = \frac{A - 2 \pm \sqrt{A(9A - 8)}}{2}, \quad (8.85)$$

must both be *real* and *negative*. Thus, the stability criterion is

$$\frac{8}{9} \leq A \leq 1. \quad (8.86)$$

Figure 8.13 shows A calculated at the three co-linear Lagrange points as a function of μ_2 , for all allowed values of this parameter (i.e., $0 < \mu_2 \leq 0.5$). It can be seen that A is always greater than unity for all three points. Hence, we conclude that the co-linear Lagrange points, L_1 , L_2 , and L_3 , are intrinsically unstable equilibrium points in the co-rotating frame.

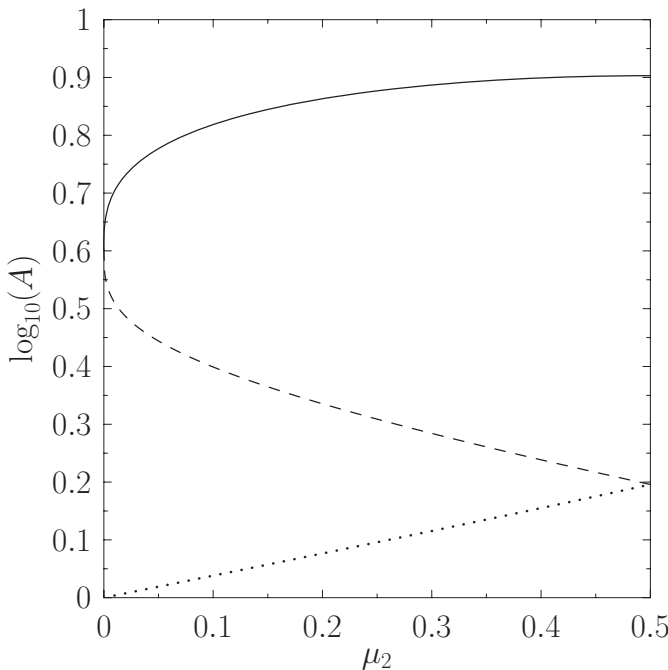


Fig. 8.13 The solid, dashed, and dotted curves show A as a function of μ_2 at L_1 , L_2 , and L_3 Lagrange points, respectively.

Let us now consider the triangular Lagrange points, L_4 and L_5 . These points are characterized by $\rho_1 = \rho_2 = 1$. It follows that $A = 1$, $B = 9/4$, $C = \pm\sqrt{27/16}(1 - 2\mu_2)$, and $D = 3/4$. Hence, $U_{xx} = -3/4$, $U_{yy} = -9/4$, and $U_{xy} = \mp\sqrt{27/16}(1 - 2\mu_2)$, where the upper and lower signs correspond to L_4 and L_5 , respectively. Equation (8.76) thus yields

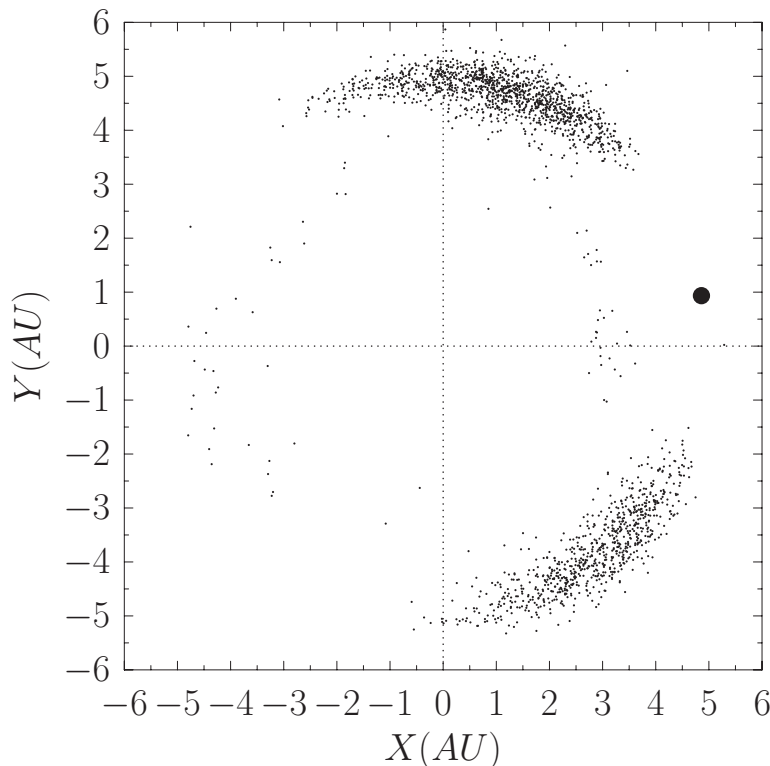
$$\Gamma^2 + \Gamma + \frac{27}{4}\mu_2(1 - \mu_2) = 0 \quad (8.87)$$

for both points, where $\Gamma = \gamma^2$. As before, the stability criterion is that the two roots of the preceding equation must both be real and negative. This is the case provided that $1 > 27\mu_2(1 - \mu_2)$, which yields the stability criterion

$$\mu_2 < \frac{1}{2} \left(1 - \sqrt{\frac{23}{27}} \right) = 0.0385. \quad (8.88)$$

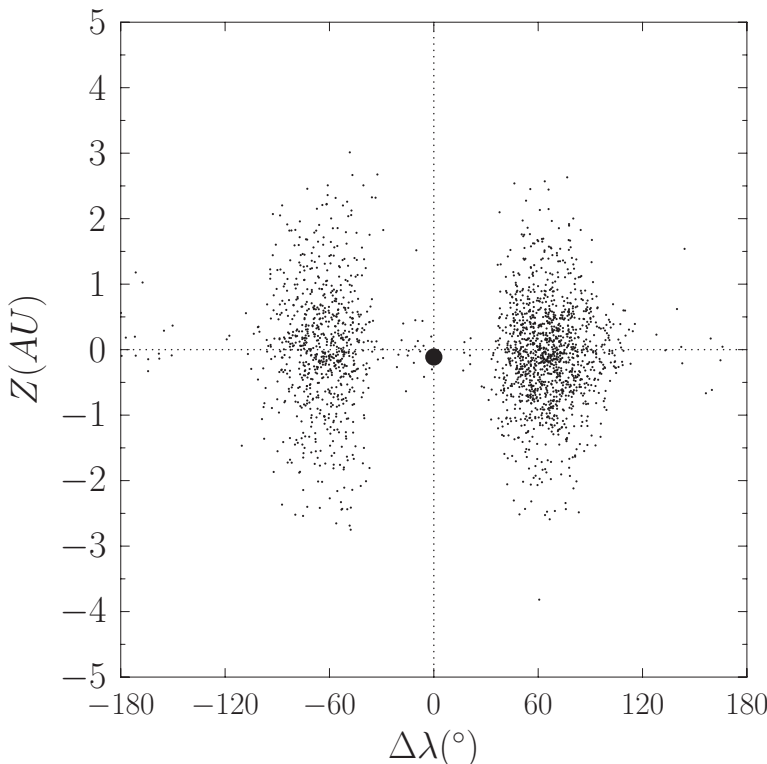
In unnormalized units, this criterion becomes

$$\frac{m_2}{m_1 + m_2} < 0.0385. \quad (8.89)$$

**Fig. 8.14**

Positions of the Trojan asteroids (small circles) and Jupiter (large circle) projected onto ecliptic plane (viewed from the north) at MJD 55600. The X -axis is directed toward the vernal equinox. Raw data from JPL Small-Body Database.

We thus conclude that the L_4 and L_5 Lagrange points are stable equilibrium points, in the co-rotating frame, provided that mass m_2 is less than about 4 percent of mass m_1 . If this is the case, then mass m_3 can orbit around these points indefinitely. In the inertial frame, the mass will share the orbit of mass m_2 about mass m_1 , but it will stay approximately 60° *ahead* of mass m_2 if it is orbiting the L_4 point, or 60° *behind* if it is orbiting the L_5 point. (See Figure 8.12.) This type of behavior has been observed in the solar system. For instance, there is a subclass of asteroids, known as the *Trojan asteroids*, that are trapped in the vicinity of the L_4 and L_5 points of the Sun–Jupiter system [which easily satisfies the stability criterion in Equation (8.89)], and consequently share Jupiter’s orbit around the Sun, staying approximately 60° ahead of and 60° behind Jupiter, respectively. These asteroids are shown in Figures 8.14 and 8.15. The Sun–Jupiter system is not the only dynamical system in the solar system that possesses Trojan asteroids trapped in the vicinity of its L_4 and L_5 points. In fact, the Sun–Neptune system has eight known Trojan asteroids, the Sun–Mars system has four, and the Sun–Earth system has one (designated 2010 TK7) trapped at the L_4 point. The L_4 and L_5 points of the Sun–Earth system are also observed to trap clouds of interplanetary dust.

**Fig. 8.15**

Positions of the Trojan asteroids (small circles) and Jupiter (large circle) at MJD 55600. Z is normal distance from the ecliptic plane. $\Delta\lambda$ is the difference in ecliptic longitude between the asteroids and Jupiter. Raw data from JPL Small-Body Database.

Exercises

- 8.1** Demonstrate directly from Equations (8.5)–(8.7) and (8.11)–(8.13) that the Jacobi integral C , which is defined in Equation (8.10), is a constant of the motion in the circular restricted three-body problem.
- 8.2** A comet approaching the Sun in a parabolic orbit of perihelion distance r_p and inclination I (with respect to Jupiter's orbital plane) is disturbed by a close encounter with Jupiter such that its orbit is converted into an ellipse of major radius a' , eccentricity e' , and inclination I' . Demonstrate that

$$\sqrt{2r_p} \cos I \simeq \frac{1}{2a'} + \sqrt{(1-e'^2)a'} \cos I',$$

where all lengths are normalized to the major radius of Jupiter.

- 8.3** A comet approaching the Sun in a hyperbolic orbit of perihelion distance r_p and inclination I (with respect to Jupiter's orbital plane), whose asymptotes subtend an acute angle ϕ with respect to one another, is disturbed by a close encounter

with Jupiter such that its orbit is converted into an ellipse of major radius a' , eccentricity e' , and inclination I' . Demonstrate that

$$\frac{1}{2r_p}(1-e) + \sqrt{(1+e)r_p} \cos I \simeq \frac{1}{2a'} + \sqrt{(1-e'^2)a'} \cos I',$$

where $e = \sec(\phi/2)$, and all lengths are normalized to the major radius of Jupiter.

- 8.4** Let (ξ, η, ζ) be the coordinates of mass m_3 in the inertial frame, and let (x, y, z) be the corresponding coordinates in the co-rotating frame. It follows that

$$\mathbf{x} = \mathbf{A}\boldsymbol{\xi},$$

where \mathbf{x} is the column vector of the co-rotating coordinates, $\boldsymbol{\xi}$ is the column vector of the inertial coordinates, and

$$\mathbf{A} = \begin{pmatrix} \cos \omega t & \sin \omega t & 0 \\ -\sin \omega t & \cos \omega t & 0 \\ 0 & 0 & 1 \end{pmatrix}.$$

Demonstrate that $\mathbf{A}^T \mathbf{A} = \mathbf{1}$, where T denotes a transpose, and

$$\mathbf{1} = \begin{pmatrix} 1 & 0 & 0 \\ 0 & 1 & 0 \\ 0 & 0 & 1 \end{pmatrix}.$$

Hence, deduce that $\mathbf{x}^T \mathbf{x} = \boldsymbol{\xi}^T \boldsymbol{\xi}$, or $x^2 + y^2 = \xi^2 + \eta^2$.

Show that

$$\dot{\mathbf{x}} = \mathbf{A} \dot{\boldsymbol{\xi}} - \omega \mathbf{B} \boldsymbol{\xi},$$

where $\dot{\mathbf{x}}$ is the column vector of the time derivatives of the co-rotating coordinates, $\dot{\boldsymbol{\xi}}$ is the column vector of the time derivatives of the inertial coordinates, and

$$\mathbf{B} = \begin{pmatrix} \sin \omega t & -\cos \omega t & 0 \\ \cos \omega t & \sin \omega t & 0 \\ 0 & 0 & 0 \end{pmatrix}.$$

Demonstrate that

$$\dot{\mathbf{x}}^T \dot{\mathbf{x}} = \dot{\boldsymbol{\xi}}^T \mathbf{1} \dot{\boldsymbol{\xi}} - \omega \dot{\boldsymbol{\xi}}^T \mathbf{C} \boldsymbol{\xi} - \omega \dot{\boldsymbol{\xi}}^T \mathbf{C}^T \boldsymbol{\xi} + \omega^2 \dot{\boldsymbol{\xi}}^T \mathbf{1}' \boldsymbol{\xi},$$

where

$$\mathbf{1}' = \begin{pmatrix} 1 & 0 & 0 \\ 0 & 1 & 0 \\ 0 & 0 & 0 \end{pmatrix}$$

and

$$\mathbf{C} = \begin{pmatrix} 0 & 1 & 0 \\ -1 & 0 & 0 \\ 0 & 0 & 0 \end{pmatrix}.$$

Hence, deduce that

$$\dot{x}^2 + \dot{y}^2 + \dot{z}^2 = \dot{\xi}^2 + \dot{\eta}^2 + \dot{\zeta}^2 - 2\omega(\xi\dot{\eta} - \eta\dot{\xi}) + \omega^2(\xi^2 + \eta^2).$$

Finally, show that the Jacobi constant in the co-rotating frame,

$$C = 2\left(\frac{\mu_1}{\rho_1} + \frac{\mu_2}{\rho_2}\right) + \omega^2(x^2 + y^2) - \dot{x}^2 - \dot{y}^2 - \dot{z}^2,$$

transforms to

$$C = 2\left(\frac{\mu_1}{\rho_1} + \frac{\mu_2}{\rho_2}\right) + 2\omega(\xi\dot{\eta} - \eta\dot{\xi}) - \dot{\xi}^2 - \dot{\eta}^2 - \dot{\zeta}^2$$

in the inertial frame.

- 8.5** Derive the first three terms (on the right-hand side) of Equation (8.46) from Equation (8.45), and the first three terms of Equation (8.47) from Equation (8.46).
- 8.6** Derive the first three terms of Equation (8.50) from Equation (8.49), and the first three terms of Equation (8.51) from Equation (8.50).
- 8.7** Derive the first two terms of Equation (8.53) from Equation (8.52), and the first two terms of Equation (8.54) from Equation (8.53).
- 8.8** Derive Equations (8.62)–(8.66).
- 8.9** Employing the standard system of units for the circular restricted three-body problem, the equation defining the location of a zero-velocity curve in the x – y plane of the co-rotating frame is

$$C = x^2 + y^2 + 2\left(\frac{\mu_1}{\rho_1} + \frac{\mu_2}{\rho_2}\right),$$

where C is the value of the Jacobi constant, and $\rho_1 = [(x + \mu_2)^2 + y^2]^{1/2}$ and $\rho_2 = [(x - \mu_1)^2 + y^2]^{1/2}$ are the distances to the primary and secondary masses, respectively. The critical zero-velocity curve that passes through the L_3 point, when $C \approx 3 + \mu_2$, has two branches. Defining polar coordinates such that $x = r \cos \theta$ and $y = r \sin \theta$, show that when $\mu_2 \ll 1$ the branches intersect the unit circle $r = 1$ at $\theta = \pi$ and $\theta = \pm 23.9^\circ$. (Modified from Murray and Dermott 1999.)

- 8.10** In the circular restricted three-body problem (employing the standard system of units) the condition for the three co-linear Lagrange points to be linearly unstable is $A > 1$, where $A = \mu_1/\rho_1^3 + \mu_2/\rho_2^3$. Here, ρ_1 and ρ_2 are the distances to the masses μ_1 and μ_2 , respectively. Let $\alpha = (\mu_2/3\mu_1)^{1/3}$ and $\beta = (7/12)(\mu_2/\mu_1)$. Consider the limit $\mu_2 \rightarrow 0$. Show that close to L_1 , where $\rho_2 \approx \alpha - \alpha^2/3$ and $\rho_1 = 1 - \rho_2$, the parameter A takes the value $A \approx 4 + 6\alpha + \mathcal{O}(\alpha^2)$. Likewise, show that close to L_2 , where $\rho_2 \approx \alpha + \alpha^2/3$ and $\rho_1 = 1 + \rho_2$, the parameter A takes the value $4 - 6\alpha + \mathcal{O}(\alpha^2)$. Finally, show that close to L_3 , where $\rho_1 \approx 1 - \beta$ and $\rho_2 = 1 + \rho_1$, the parameter A takes the value $1 + (3/2)\beta + \mathcal{O}(\beta^2)$. Hence, deduce that the three co-linear Lagrange points are all linearly unstable. Demonstrate that, in the case of the L_3 point, the growth-rate of the fastest growing instability is $\gamma \approx [\sqrt{(21/8)\mu_2} + \mathcal{O}(\mu_2)]\omega$. (Modified from Murray and Dermott 1999.)
- 8.11** Consider the circular restricted three-body problem. Demonstrate that if $[x(t), y(t), z(t)]$ is a valid trajectory for m_3 in the co-rotating frame, then $[x(t), y(t), -z(t)]$ and $[x(-t), -y(-t), z(-t)]$ are also valid trajectories. Show that if $[x(t), y(t), z(t)]$

is a valid trajectory when $\mu_2 = \zeta$ (where $0 \leq \zeta \leq 1$), then $[-x(t), -y(t), z(t)]$ is a valid trajectory when $\mu_2 = 1 - \zeta$.

- 8.12** Consider the circular restricted three-body problem (adopting the standard system of units). Suppose that $\mu_2 \ll 0.0385$, so that the L_4 and L_5 points are stable equilibrium points (in the co-rotating frame) for the tertiary mass. Consider motion (in the co-rotating frame) of the tertiary mass in the vicinity of L_4 that is confined to the x - y plane. Let

$$\begin{aligned} x &= \frac{1}{2} - \mu_2 + \delta x, \\ y &= \frac{\sqrt{3}}{2} + \delta y, \end{aligned}$$

where $|\delta x|, |\delta y| \ll 1$. It is helpful to rotate the Cartesian axes through 30° , so that

$$\begin{pmatrix} \delta x \\ \delta y \end{pmatrix} = \begin{pmatrix} \sqrt{3}/2 & 1/2 \\ -1/2 & \sqrt{3}/2 \end{pmatrix} \begin{pmatrix} \delta x' \\ \delta y' \end{pmatrix}.$$

Thus, $\delta x'$ parameterizes displacements from L_4 that are *tangential* to the unit circle on which the mass m_2 and the L_3 , L_4 , and L_5 points lie, whereas $\delta y'$ parameterizes *radial* displacements. Writing $\delta x'(t) = \delta x'_0 \exp(\gamma t)$ and $\delta y'(t) = \delta y'_0 \exp(\gamma t)$, where $\delta x'_0, \delta y'_0, \gamma$ are constants, demonstrate that

$$\begin{pmatrix} \sqrt{3}\gamma^2/2 + \gamma - 3\sqrt{3}\mu_2/4 & \gamma^2/2 - \sqrt{3}\gamma - 3/2 + 9\mu_2/4 \\ -\gamma^2/2 + \sqrt{3}\gamma + 9\mu_2/4 & \sqrt{3}\gamma^2/2 + \gamma - 3\sqrt{3}/2 + 3\sqrt{3}\mu_2/4 \end{pmatrix} \begin{pmatrix} \delta x'_0 \\ \delta y'_0 \end{pmatrix} = \begin{pmatrix} 0 \\ 0 \end{pmatrix},$$

and, hence, that

$$\gamma^4 + \gamma^2 + \frac{27}{4}\mu_2(1 - \mu_2) = 0.$$

Show that the general solution to the preceding dispersion relation is a linear combination of two normal modes of oscillation, and that the higher-frequency mode takes the form

$$\begin{aligned} \delta x'(t) &\simeq -2e \sin(\omega_+ t - \phi_+), \\ \delta y'(t) &\simeq -e \cos(\omega_+ t - \phi_+), \end{aligned}$$

where

$$\omega_+ \simeq \left(1 - \frac{27}{8}\mu_2\right)\omega,$$

and e, ϕ_+ are arbitrary constants. Demonstrate that, in the original inertial reference frame, the addition of the preceding normal mode to the unperturbed orbit of the tertiary mass (in the limit $0 < e \ll 1$) converts a circular orbit into a Keplerian ellipse of eccentricity e . In addition, show that the perihelion point of the new orbit precesses (in the direction of the orbital motion) at the rate

$$\dot{\varpi} = \frac{27}{8}\mu_2\omega.$$

Demonstrate that (in the co-rotating reference frame) the second normal mode takes the form

$$\delta x'(t) \simeq d \sin(\omega_- t - \phi_-),$$

$$\delta y'(t) \simeq -\sqrt{3\mu_2} d \sin(\omega_- t - \phi_-),$$

where

$$\omega_- \simeq \frac{3}{2} \sqrt{3\mu_2} \omega,$$

and d, ϕ_- are arbitrary constants. This type of motion, which entails relatively small-amplitude radial oscillations, combined with much larger-amplitude tangential oscillations, is known as *libration*.

Finally, consider a Trojan asteroid trapped in the vicinity of the L_4 point of the Sun–Jupiter system. Demonstrate that the libration period of the asteroid (in the co-rotating frame) is approximately 148 years, whereas its perihelion precession period (in the inertial frame) is approximately 3,690 years. Show that, in the co-rotating frame, the libration orbit is an ellipse that is elongated in the direction of the tangent to the Jovian orbit in the ratio 18.7:1.